Journal of Neuroscience Methods 293 (2018) 183–190

Contents lists available at ScienceDirect

Journal of Neuroscience Methods

journal homepage: www.elsevier.com/locate/jneumeth

Research article

A 3D-printed modular device for imaging the brain of small birds

Christine R. Lattin[a,*], Maxwell A. Emerson[b], Jean-Dominique Gallezot[a], Tim Mulnix[a], J. Elliott Brown[a], Richard E. Carson[a]

[a] *Department of Radiology and Biomedical Imaging, Yale University, New Haven, CT, USA*
[b] *Yale Center for Engineering, Innovation & Design, Yale University, New Haven, CT, USA*

HIGHLIGHTS

- *In vivo* CT, PET and MRI imaging of any new species requires new equipment.
- We describe the design and use of a 3D-printed device for imaging the songbird brain.
- Use of this device significantly improved positional reproducibility of the head.
- 3D-printed materials are also imaging-compatible and fast and inexpensive to make.
- Researchers can use our design and CAD models for fabricating their own devices.

ARTICLE INFO

Article history:
Received 26 June 2017
Received in revised form
18 September 2017
Accepted 5 October 2017
Available online 6 October 2017

Keywords:
3D printing
Small animal imaging
CAD
Positron emission tomography
Computed tomography

ABSTRACT

Background: One potential barrier to using *in vivo* imaging in any new animal species is solving the basic problem of how to hold animals safely and securely during scans.
New method: In this paper, we describe the design, fabrication, use, and positional reproducibility of a 3D-printed plastic device (the Avian Imaging Device, or AID) for imaging the brain of 1 or 2 small songbirds. We designed two different types of head cones to use with this device: one that was not contoured and designed for anesthesia induction, and one contoured to the shape of a house sparrow head, designed to be used with a pre-anesthetized animal.
Results: Compared to no holder, using the AID with both contoured and non-contoured head cones significantly reduced the amount of translation necessary to align the head in pairs of CT scans (by 78% and 90%, respectively); using the contoured head cone also significantly reduced the amount of rotation necessary for head alignment in registering pairs of scans (by 90%).
Comparison with existing method(s): Using an animal holder that can not only securely hold animals but which has high positional reproducibility is essential to take advantage of the maximum resolution possible with small animal imaging. 3D-printed materials are also compatible with PET and CT, environmentally stable, and fast and inexpensive to make.
Conclusions: Researchers can learn from the design of the AID and use our CAD models as a starting point for fabricating devices for multiple small-animal imaging needs.

1. Introduction

As the resolution of computed tomography (CT), positron emission tomography (PET) and magnetic resonance imaging (MRI) has improved, there has been a proliferation of research using these technologies in small animals (Doty et al., 2007; Riemann et al., 2008; Schambach et al., 2010; Souza et al., 2011). Similarly, researchers in the fields of comparative anatomy, behavioral neuroscience and sensory ecology have just started to realize the potential of using medical imaging in wild animals, and recent studies have used PET, CT and MRI to examine neural activity in American crows (*Corvus brachyrhynchos*) exposed to different visual stimuli (Marzluff et al., 2012), antipredator behavior in the Spanish ribbed newt (*Pleurodeles waltl*) (Heiss et al., 2010) and testosterone effects on brain nuclei in European starlings (*Sturnus vulgaris*) (Van Meir et al., 2004). These technologies have a number of potential advantages over many existing techniques for studying the brain and body. Because medical imaging does not require euthanizing animals, it can be used with longitudinal study designs,

* Corresponding author at: Positron Emission Tomography Center, Yale University, 801 Howard Avenue, PO Box 208048, New Haven, CT 06520-8048, USA.
E-mail address: christine.lattin@yale.edu (C.R. Lattin).

https://doi.org/10.1016/j.jneumeth.2017.10.005

allowing animals to serve as their own controls. This can be especially important due to the large individual variation that exists in many physiological systems in wild animals (Williams, 2008), or where there may be complex interactions between experimental treatments and time. For example, in the European starling study mentioned above (Van Meir et al., 2004), *ex vivo* histological analysis did not reveal any group differences in brain nuclei size between testosterone-treated and control animals; differences only became apparent using within-animal repeated imaging with MRI. Also, the effects of these technologies on subjects can be minimal, allowing animals to be released back into the wild after scanning, as was done with the crows in the project mentioned above.

Because most small animal imaging is done on laboratory rodents, scanning other organisms can require an extensive process of creating new equipment to administer anesthesia, hold animals securely during scans, and reproducibly reposition them for repeat scans. However, it can be challenging to design equipment customized to new animal species for several reasons. First, these imaging technologies create restrictions against using materials such as metal, which is unsafe to use with MRI and causes artifacts in CT images (Boas and Fleischmann, 2012). Secondly, using conventional manufacturing processes like lathes to create one-of-a-kind equipment can be both time-consuming and expensive. 3D printing provides an inexpensive, widely available alternative to conventional manufacturing in a material (plastic) that works well with all medical imaging modalities (Herrmann et al., 2014).

Songbirds have long been an important model system for research in areas as diverse as vocal learning (Brainard and Doupe, 2013), visual processing (Rogers, 1996) and stress (Rich and Romero, 2005), and recent studies have used PET, CT and MRI to explore these and other questions in songbird models (Van der Linden et al., 2009; Cross et al., 2013; Gold et al., 2016; Louder et al., 2016; Lattin et al., 2017a,b). In this paper, we describe the design and use of a modular 3D-printed holder, the Avian Imaging Device (AID), for *in vivo* imaging of the brain of a small songbird, the house sparrow (*Passer domesticus*). We also present data showing the repeatability of head positioning using two different versions of this device, as compared to no holder, and examine PET signal losses due to holder material. The AID has several design features making it uniquely suited for imaging the brain in small birds; however, due to its modular components, the design is flexible enough to be easily adapted for use in other small animal species (all files are available as Supplemental material).

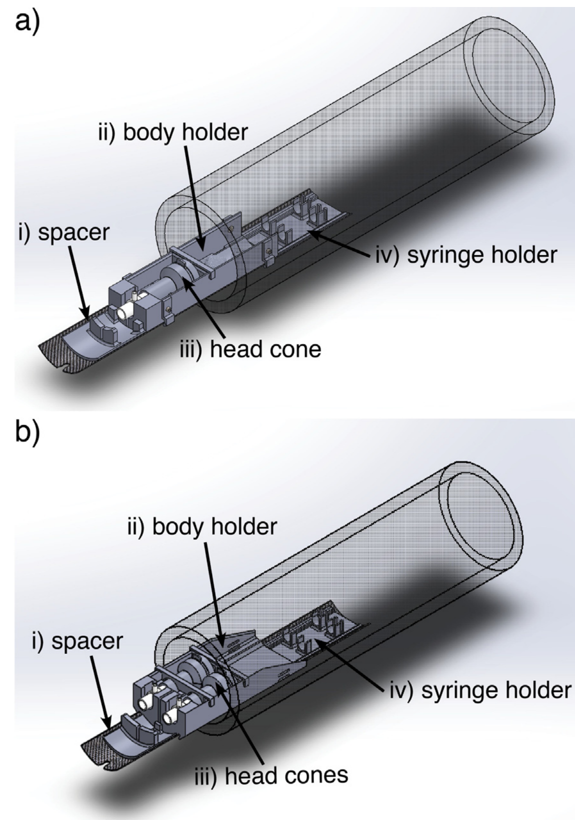

Fig. 1. a) Rendering of the 1-bird version of the Avian Imaging Device, from left to right: i) spacer, ii) body holder with iii) inserted head cone, and iv) syringe tray, demonstrating how it fits onto the 70-mm extended carbon fiber pallet and inside the bore tunnel of the Inveon (depicted as a transparent cylinder). The spacer and syringe tray attach to the body holder using tab inserts; the body holder attaches to the pallet using four screws. b) The 2-bird version of the holder uses the same spacer, head cone and syringe tray, but is wider to accommodate an additional head cone and the bodies of two birds. The body holder has slots to slide onto the pallet.

2. Materials and methods

2.1. Study subjects

House sparrows used for design and testing of the AID were caught in New Haven, CT, USA using Potter traps. House sparrows are ~15–17 cm in length, and brain diameter at the widest point is ~20 mm, similar to many other small passerines. Animal procedures were performed in accordance with the National Institutes of Health guide for the care and use of Laboratory animals (NIH Publications No. 8023, revised 1978). Animals were collected under Connecticut state permit 1417011, and all procedures approved by the Yale University Animal Care and Use Committee under protocol 2014-11648.

2.2. MicroPET-CT scanner

The AID was designed for use with the Inveon Multimodality Scanner configured to include both PET and CT (Siemens Medical Solutions USA, Inc., Malvern, PA, USA). The Inveon has a 127-mm axial field of view for PET and image resolution (full width at half maximum, FWHM) is ~1–3 mm, depending on the reconstruction technique used, distance of the scanned object to the center of the field of view, and direction (tangential, radial or axial) (Visser et al., 2009). The Inveon is one of the most widely available small-animal PET scanners; however, the AID could be easily customized for use with other scanner types by adjusting the length, width and diameter of different components.

2.3. AID design and creation: general principles

There are two versions of the AID, designed to hold either one or two small songbirds. Parts were designed based on the maximum width of the 125-mm CT system and the width and length of the Inveon's 70-mm extended pallet, with all components contoured to fit the 40.7° pallet curvature (Fig. 1).

To help design the AID, we acquired CT scans of an adult male and female sparrow. Birds were anesthetized using inhaled isoflurane at a concentration of 2.5–5%. CT acquisition was performed in step-and-shoot mode with three bed positions to capture the birds' entire bodies, and used 80 kV, 500 uA, 240 ms exposure time, and 120 projections at low magnification. For CT reconstructions, we used Siemens Inveon Acquisition Workplace software, Version 2.0 (Siemens Healthcare GmbH, Erlangen, Germany) using a Feldkamp reconstruction algorithm with 2x downsampling, the "slight" noise reduction setting, and a ramp filter.

Reconstructed CT images were imported as DICOM format into Mimics Innovation Suite version 17 (Materialise, Leuven, Belgium) for segmentation. Segmentation analyzes pixels through

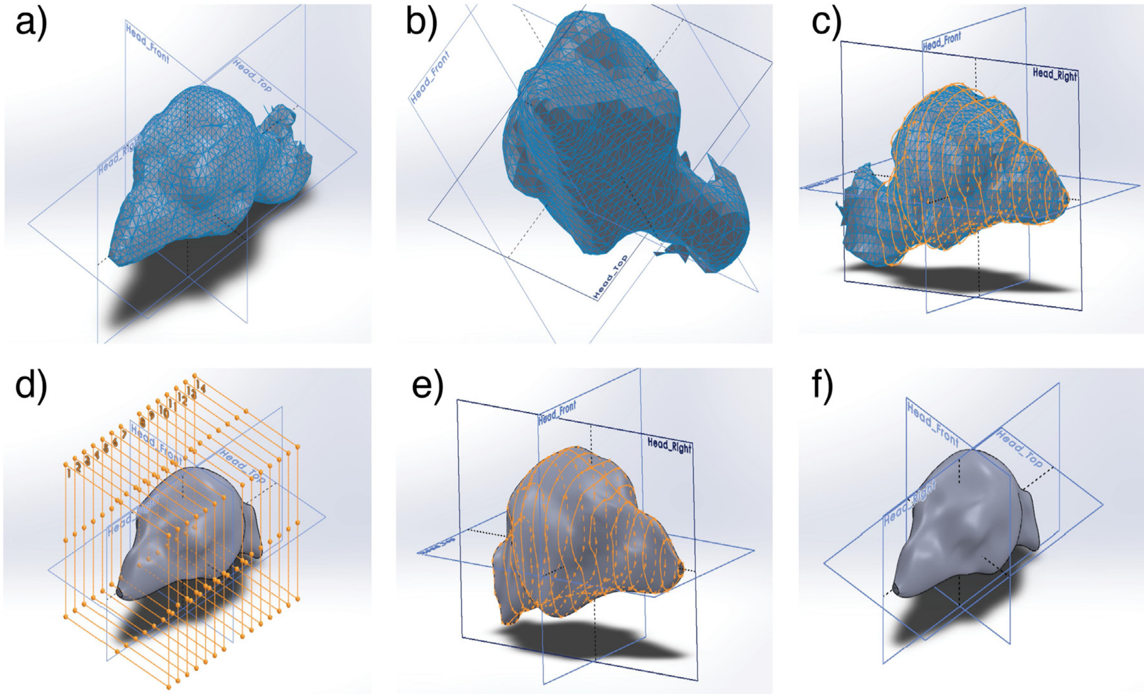

Fig. 2. a) The initial STL file of the computed tomography (CT) image imported into SolidWorks. b) A view showing extra appendages present in the STL file due to the high resolution of the CT image. c) Manual outlines of the anatomy on the STL file. d) A total of 15 parallel planes were created with 2.54 mm offset for profiles to be drawn for the SolidWorks loft feature. e) The resulting loft with the sketches of each profile shown. The loft is much smoother than the STL file. f) The final bird head loft feature used to create the contoured head cones.

multiple axial slices and assigns them to a 3D object. Using semi-automated segmentation, a 3D stereolithography (STL) file of contours of the bird's body without feathers was created. This file was imported into 3-matic version 10 (Materialise, Leuven, Belgium) and mesh errors created during the segmentation process (*e.g.*, gaps in the mesh, or intersecting triangles (Friedman et al., 2016)) were corrected. Finally, the number of triangles was reduced to be compatible with our computer-aided design (CAD) software, SolidWorks 2015 (Dassault Systèmes SolidWorks Corp., Vélizy-Villacoublay, France) (Fig. 2a).

After importing the STL files, we decided to model the head surface by creating a loft feature in SolidWorks. The STL surfaces included undesirable geometry such as small appendages that were not necessary for the overall head shape to be modeled (Fig. 2b). By manually outlining the anatomy in SolidWorks, critical dimensions of the head and body were defined, noting body parts that should be restrained or supported in the bird holder design (Fig. 2c). The scan was then cropped to serve as a model for the cavity of contoured head cones (see below), and the STL model segmented into planes offset by 2.54 mm increments from the Front Plane (Fig. 2d). Sketches were created on each of the planes where the outline of the bird head was manually traced to create profiles for a loft (Fig. 2e). Guide curves were created connecting the profiles, resulting in a solid-body head loft that we used to make the head cones (Fig. 2f).

2.4. Body holder

The body holder is the main component of the AID; head cones fit into this component, and the syringe tray and spacer attach to it *via* tabs. The 1-bird version is anchored to the pallet using four 6-32 nylon screws that are fastened into corresponding nuts, press-fitted into the holder walls (Fig. 3a, i). Adapter brackets attach the holder to the scanner pallet. The 2-bird version slides onto the pallet *via* slots in the body of the holder (Fig. 3b, i).

Sparrows needed to be held securely in a standardized position. To meet this design challenge, we chose to mimic a "bander's grip," where birds are held with their narrow necks between the fingers, and their wider heads and bodies above and below the hand, respectively. A narrow slot (or two slots, for the 2-bird version) was made in the holder for neck positioning (Fig. 3a, ii); above this is a space for the head cone and below this a place for the body. A plastic bar clips onto the holder above the neck slot (Fig. 3a, iii). Notches in the body holder allow gauze to feed through to secure birds' legs (Fig. 3b, ii). The different styles of head cones all fit into notches in the body holder; there are also holes for anesthesia tubing. For the 2-bird version, we also created a clip that anchors head cones to the body holder (Fig. 3b, iii). We use a PET/CT compatible heating pad (73.66 mm width × 146.06 mm length; m2m Imaging, Cleveland, OH, USA) to keep animals warm during scans, and notches in the body holder allow the pad and its power cord to enter *via* the top of the holder. These notches could also be used (and expanded, if necessary) to accommodate wires for other systems used to monitor body temperature, respiratory rate, and other physiological parameters. There is ample room for such additional probes in the body holder. The total length of the body holder is 21.3 cm.

2.5. Head cones

We created two different types of head cone for two different imaging scenarios. These can be used interchangeably with the other parts of the holder assembly. In the first scenario, animals were injected with radiotracers while awake and anesthetized on the scanner bed–this required a head cone that a bird could be quickly inserted into. This version was fairly large, so head positioning was not completely uniform across different scans (Fig. 4a; see also Results). One end of this cone was designed to fit a 13 mm inner diameter × 15 mm outer diameter airway adapter (Straight Airway Adapter WW1100, Surgivet, Smiths Medical PM, Inc., Norwell, MA, USA), which attached to tubing feeding in anesthesia gas,

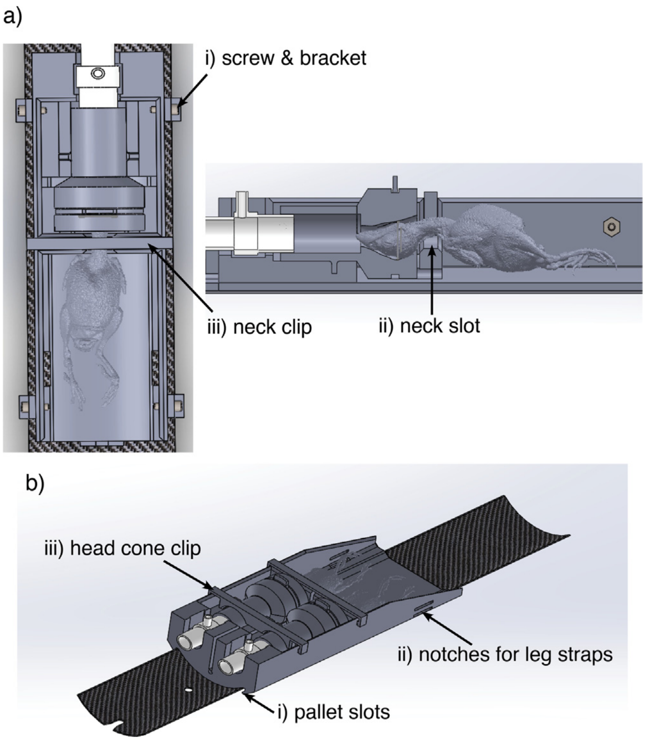

Fig. 3. a) The 1-bird body holder and contoured head cone, as viewed from the top (left) and side (right). The holder is attached to the pallet *via* 4 sets of screws and brackets (i). A house sparrow (depicted without feathers) is shown in supine position, although the head cone could also be rotated 180° or 90° to allow for prone or side positioning, respectively. The non-contoured version of the head cone and body holder allows for any body positioning. The bird's neck fits into a slot in the body holder (ii), and is secured using a clip (iii), although no pressure is put on the bird at this point. Anesthesia feeds into the head cone from tubing that attaches to the white component, which is a standard airway adapter (see '*Head cones*' for more details). b) The 2-bird body holder and head cones, viewed at an angle. The 2-bird holder fits onto the pallet with slots (i). The bird's legs may be secured using a gauze strip that passes through notches in the bird holder (ii). Head cones are anchored using a clip that attaches to the body holder (iii).

with a separate exhaust outlet for waste anesthesia gases (F/AIR canisters, A. M. Bickford, Wales, NY, USA). The other end of the cone was open and designed to be covered by latex sheets with slots cut into them for insertion of the animal's head. In cases where an animal's head needs to be tightly fixed to avoid movement artifacts, this non-contoured version of the head cone could also support additional ear bar or beak fixation components (*e.g.*, Van Meir et al., 2005), as long as they were not too large. Using this non-contoured head cone, animals could be scanned in supine or prone position or on their sides.

In the second imaging scenario, animals were anesthetized elsewhere and then transferred to the scanner bed. This head cone consisted of two interlocking parts, and was contoured to sparrows' head shape to minimize variation in positioning (Fig. 4b). Using the head loft previously described, contoured head cones were created by generating a cavity in the cone with a 10% scaling offset from the model for the "male" version, and a 5% offset for the "female" version. This made the cavity slightly bigger than the solid features of the head to account for feathers and slight variations in bird-to-bird anatomy. In cases where very rigid fixation is necessary, customized contoured head cones could be made from CT images of each individual animal to be scanned, using the method described above. These head cones were split along the midline with grooves for aligning the two pieces. After the anesthetized bird was positioned, the two halves were secured using surgical tape at the seams, which also effectively sealed the cones to minimize anesthesia leakage. By rotating the contoured head cone, investigators can position animals in supine or prone position, or on their sides. Representative images from PET scans using the non-contoured and contoured head cones are shown in Fig. 5, and show no indication of PET artifacts.

2.6. Spacer

PET sensitivity is highest in the center of the field of view (in the axial direction), and because we were primarily interested in brain imaging, the brain could be placed in the center of the field of view. However, we faced a tradeoff between sensitivity and fitting the animal's whole body in the field of view to confirm injected dose and examine radiotracer binding in other tissues. We chose to position the bird's whole body in the field of view except for the legs, which allowed us to place the brain fairly close to the axial center of the field of view, but also image most of the bird's body. To consistently achieve this placement, we created a 77.2 mm-long spacer with a plastic tab that fit into the top of the body holder (Fig. 6). This was designed to press flush against the top of

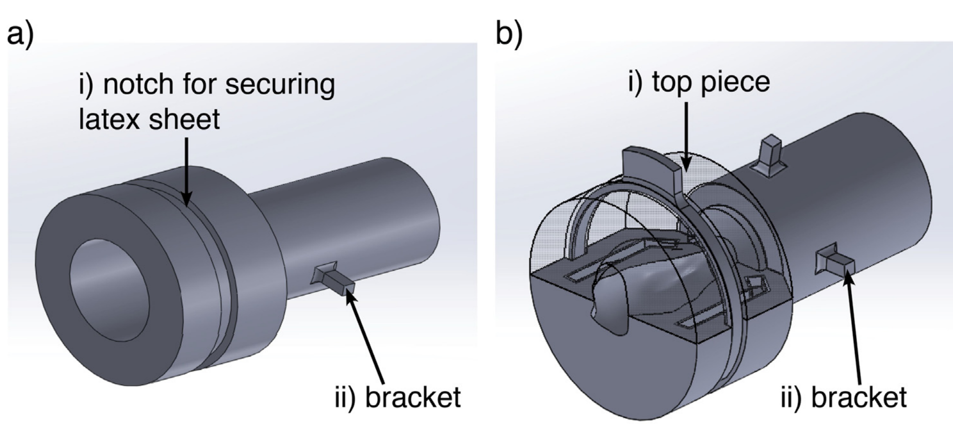

Fig. 4. Two different head cones designed for use with the Avian Imaging Device. a) One version is not contoured and was designed for anesthesia induction. It is one solid piece covered at the end with a piece of latex, which is secured using a rubber band that fits into the notch in the cone (i). b) The other version is contoured to the shape of a house sparrow head, designed to use with a pre-anesthetized animal. The contoured head cone is made of two interlocking pieces (the top piece, i, is rendered as transparent), and the two pieces joined together using surgical tape at the seams. For both versions of the head cone, anesthesia tubing feeds in from the right, and the cone sits into the body holder using 4 square brackets (ii) that fit into corresponding notches in the holder to allow positioning birds in prone or supine position or on their sides.

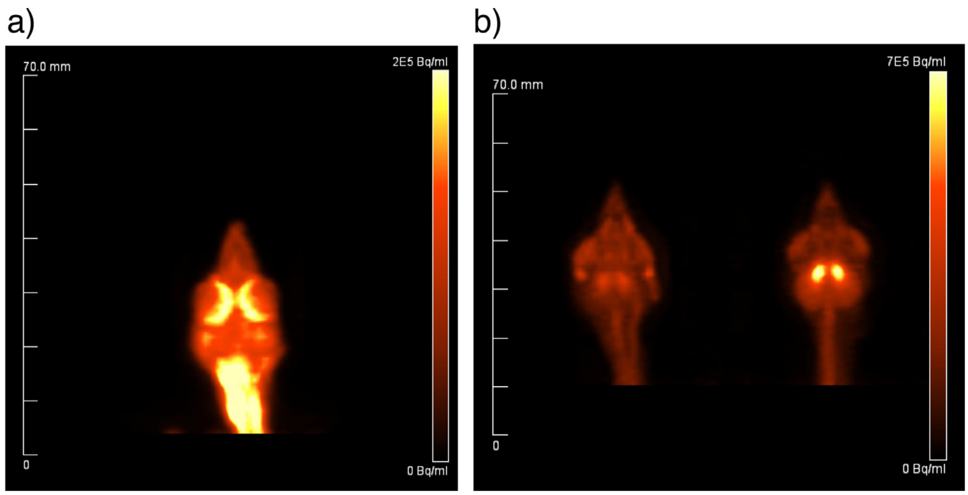

Fig. 5. Representative positron emission tomography (PET) maximum intensity projection images of house sparrow brain made using the Avian Imaging Device. a) A 30-min static image of a bird injected with ^{18}F-fluorodeoxyglucose while awake, then anesthetized and scanned using the 1-bird holder with the non-contoured head cone. b) A 60-min static image of two birds injected with ^{11}C-raclopride while under anesthesia, scanned using the 2-bird holder with contoured head cones.

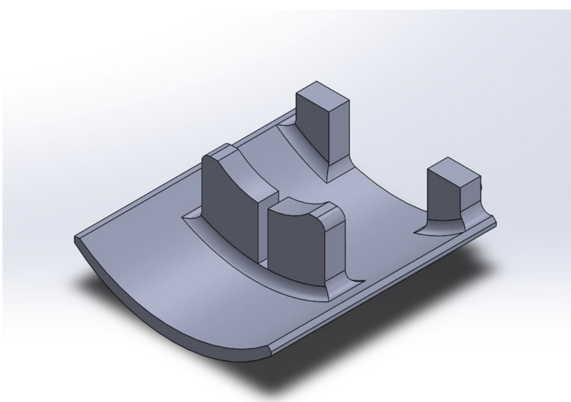

Fig. 6. A spacer that fits into the top of the Avian Imaging Device, used to consistently position the holder from scan to scan (the top of the spacer rests flush against the top of the scanner gantry). The length of the spacer was chosen to move animals' brains close to the axial center of the field of view, but still allow for whole-body imaging. This spacer also supports the anesthesia tubing feeding out from the head cones, and contains a notch for the heating pad wire.

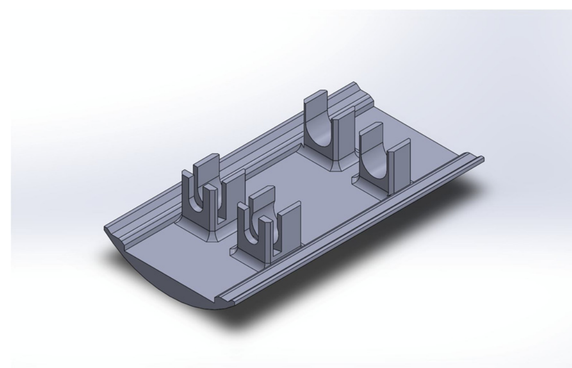

Fig. 7. A tray designed to hold two syringes for administering PET tracers or drugs during scanning, which fits into the bottom of the Avian Imaging Device.

the pallet. If we wished to change the center of the field of view, spacers of larger or smaller length could easily be created.

2.7. Syringe holder

To hold syringes for administering PET radiotracers and other drugs, we designed a tray that attached to the bottom of the body holder using another set of tabs (Fig. 7). The tray was designed to accommodate two syringes, and measured ~12 × 6 cm. This set-up allowed us to start the scanner, inject radiotracers and acquire PET data for the whole time period from pre-injection to post-injection. This is necessary to use quantitative PET kinetic modeling methods such as the simplified reference tissue model (Lammertsma and Hume, 1996).

2.8. 3D printer

All components were printed on a Dimension Elite 3D printer (Stratasys, Dimension Elite, Eden Prairie, MN, USA). The build plate size of the printer was 203 × 203 × 305 mm. All parts were printed with a 0.254 mm layer thickness out of Stratasys's Acrylonitrile Butadiene Styrene plastic material (ABSplus). For support material, their proprietary soluble support material (P400-SR) was used. With the Dimension Elite printer driver, Catalyst 4.3, the option for infill density was specified as 'SPARSE – low density'. After printing, the parts were submerged in a sodium hydroxide bath (Stratasys product) to dissolve the supports, then placed in a water bath for 9 h to let any remaining lye leach prior to use.

3. PET imaging performance

Objects in the scanner cause loss of counts due to photon attenuation. To estimate PET signal losses due to the AID for a typical scan, 2D (non-oblique) attenuation correction factor (ACF, values ≥ 1) sinograms were created by forward projections of two bird CT images, one with the AID in place and one with the AID digitally removed from the images. A *ratio* sinogram of these two ACF sinograms (with/without) was then formed to quantify increases in attenuation due to holder material. PET *loss fractions* were calculated as 1-1/ACF. The mean and standard deviation of these loss fractions were tabulated over the sinogram bins corresponding to projections passing through the bird head.

4. Reproducibility of head positioning

To quantify the reproducibility of head positioning using the AID with two different types of head cones *vs.* no holder, we used data from 17 pairs of CT scans (34 scans total), where the same subject was scanned two or more times using the same configuration: contoured head holder: n = 6 pairs; non-contoured head holder: n = 7 pairs; no holder: n = 4 pairs. CT scans were conducted and images reconstructed as described above. The AID was removed from the scanner bed and repositioned between scans. CT images were cropped around the entire head and manually coregistered using rigid transformations allowing for translation and rotation in the x, y and z directions. Images were aligned using the skull (including eye sockets) and beak, which are visualized easily in CT imaging due to the high density of these tissues. Coregistration matrices for the different image pairs were generated using tools written in IDL (Exelis Visual Information Solutions, Inc., Melbourne, Florida, USA), and used to compute two values: 1) the 3D translation distance (in mm) of the location of a reference point in the middle of the brain between the two scans, and 2) the angle of rotation (in degrees) necessary to align the two images (any rotation in 3D space can be described by its axis of rotation and one angle; this angle was calculated by converting the transformation matrices to quaternions). Because Levene's test indicated heterogeneity of variances in both translation and rotation measures among the three sets of scans (Levene 1960), we used Welch's ANOVA, with Student's *t*-tests as post-hoc tests. All statistical tests were conducted using JMP Pro 11. Images demonstrating initial differences in positioning between scans were generated using Siemens Inveon Research Workplace software, Version 2.0.

5. Results

PET signal loss fraction mean and standard deviation in head images due to the additional attenuating material of the 1-bird holder (for a typical scan) were 13 ± 2%. For the 2-bird holder, the values were 17 ± 5%. Thus, the impact of the AID on PET count efficiency is minor.

The 3D translation distance to align CT image pairs differed significantly among different scan conditions (Figs. 8a and 9 ; $F_{2,6}$ = 5.7, p = 0.027), with post-hoc tests indicating that the translation distance with no holder was greater than that with both the contoured and non-contoured head cones (no holder *vs.* contoured head cone: t = 5.0, df = 14, p = 0.0002; non-contoured head cone *vs.* contoured head cone: t = 0.77, df = 14, p = 0.46; non-contoured head cone *vs.* no holder: t = −4.5, df = 14, p = 0.0005).

The amount of rotation necessary to align image pairs also differed significantly among different scan conditions (Figs. 8b and 9 ; $F_{2,5}$ = 5.4, p = 0.0091). Post-hoc tests indicated that the amount of rotation with no holder and the non-contoured head cone was greater than that with the contoured head cone (no holder *vs*. contoured head cone: t = 2.5, df = 14, p = 0.027; non-contoured head cone *vs*. contoured head cone: t = 3.2, df = 14, p = 0.007; non-contoured head cone *vs*. no holder: t = 0.26, df = 14, p = 0.80).

6. Discussion

In this paper, we describe the design, fabrication, use, PET imaging performance and positional reproducibility of a 3D-printed device for imaging the brain of 1 or 2 small songbirds during PET and CT scans. Using the AID with both the contoured and non-contoured head cones significantly reduced the amount of translation necessary to align the head in pairs of CT scans (by 78% and 90%, respectively); using the contoured head cone also significantly reduced the amount of rotation necessary for head alignment in pairs of scans (by 90%). Because spatial resolution decreases from the center of the field of view, high positional reproducibility is essential to take advantage of the maximum possible resolution with small animal imaging and reduce partial volume error (Kessler et al., 1984). Furthermore, use of this device resulted in only modest PET count losses due to addition attenuating material, as shown by our PET losses measure. Although numerous devices have been designed to hold small animals during different *in vivo* imaging procedures, these are typically made for laboratory rodents (Cheng et al., 2009; Yagi et al., 2014), and employ design features not compatible with the anatomy of wild species used in ecological research (*e.g.*, rodent "bite bars" are not compatible with avian anatomy). To our knowledge, our use of CT imaging to design a customized head cone based on the actual shape, size and features of the house sparrow skull is unique, although this particular approach could be used in any species.

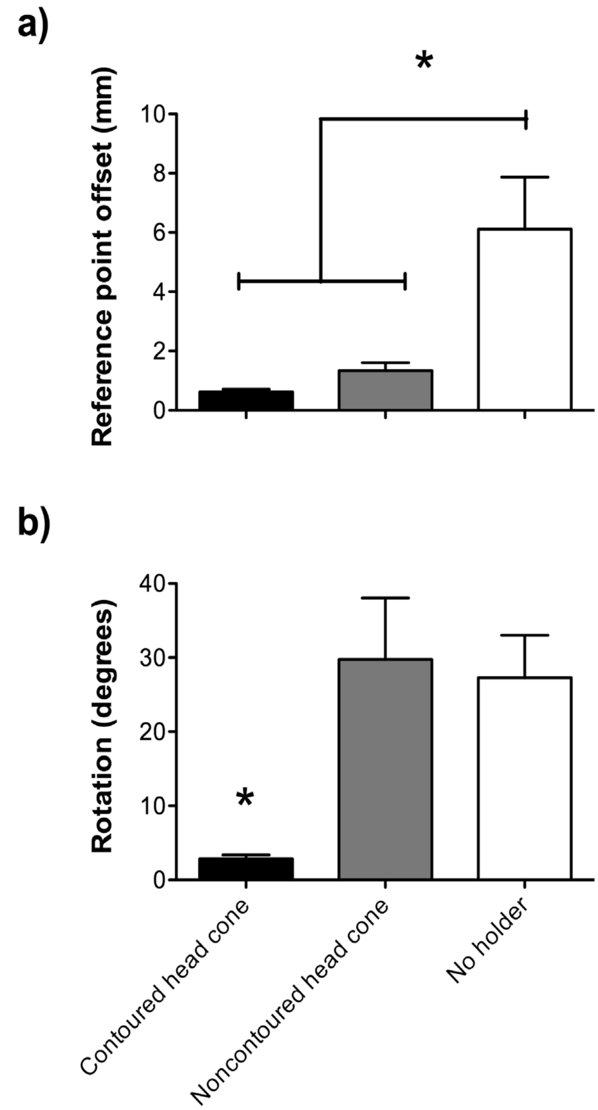

Fig. 8. Amount of a) translation (reference point offset, in mm) and b) rotation (in degrees) necessary to align two computed tomography (CT) images of the heads of the same animal using either no bird holder (n = 4 pairs of scans), or one of two different versions of the Avian Imaging Device: a version with a non-contoured head cone (n = 7 pairs of scans), or one with a contoured head cone based on CT images of house sparrows (n = 6 pairs of scans). Error bars represent SEM; stars indicate significant differences between groups using Student's *t*-tests.

3D-printed materials are inherently compatible with PET and CT, and they are also fast to fabricate–printing all parts of the AID took less than two days. The ABSplus plastic that we used, as well as other commonly used 3D printing plastics like polymerized lactic acid (PLA), are resistant to common disinfectants and environmentally stable over time (Novakova-Marcincinova and

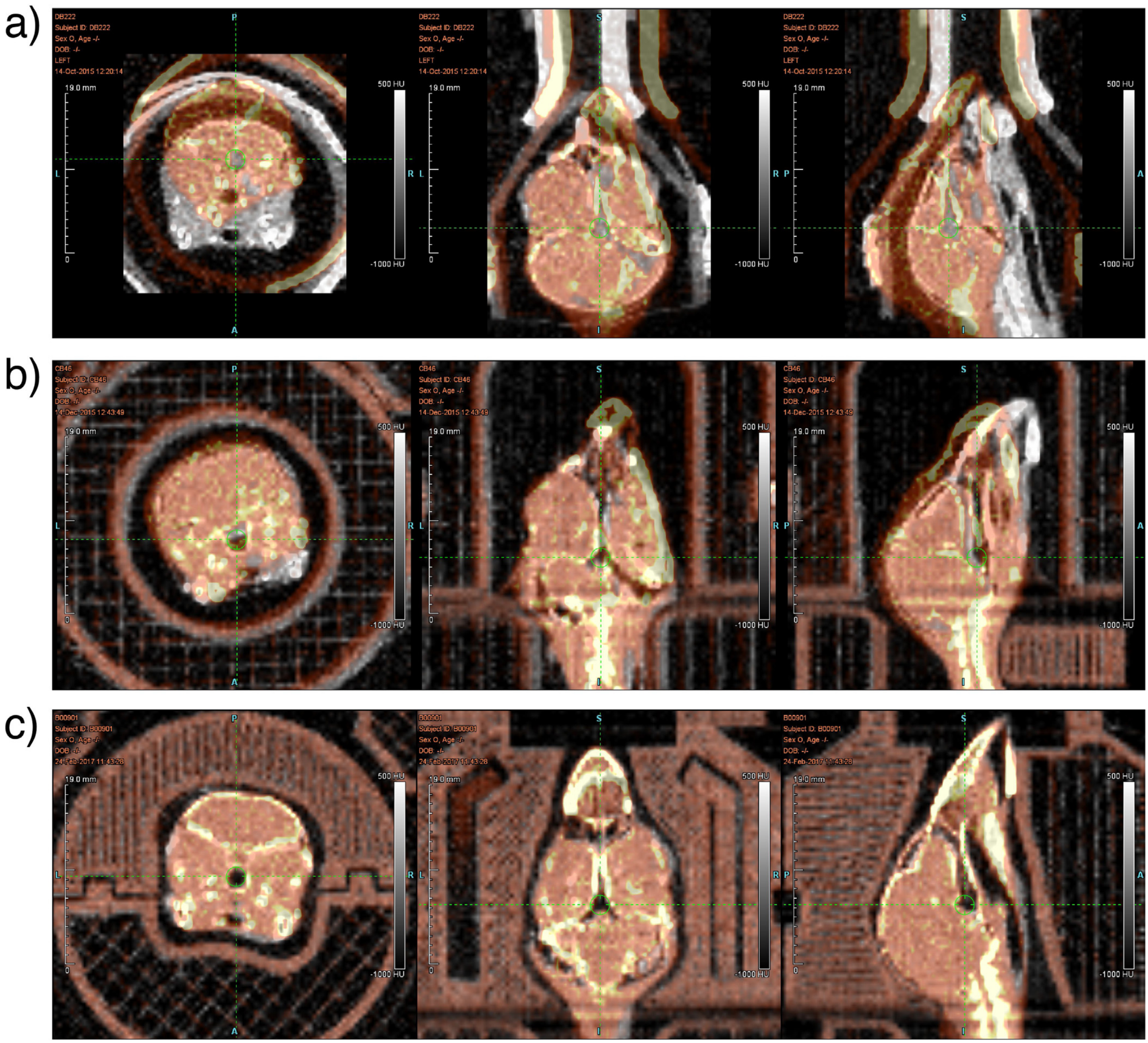

Fig. 9. Two overlaid computed tomography (CT) images, one using a grey scale and the other a red scale, demonstrating a typical amount of translation and rotation between scans of the same animal using no holder (a), using the bird holder with a non-contoured head cone (b) and using the bird holder with a contoured head cone (c). The amount of translation (reference point offset, in mm) and rotation (in degrees) necessary to align each pair of images was 4.6 mm and 29° for a; 1.7 mm and 16° for b; and 0.5 mm and 2° for c. Left to right: axial, coronal, and sagittal views.

Novak-Marcincin, 2013; Herrmann et al., 2014). Although the costs of 3D printers themselves are substantial, the raw materials used in these printers cost very little, and design features can be easily altered and prototypes re-printed as needed–we printed several versions of the AID before arriving at the final design. Even if a researcher's home institution does not have 3D printers, several companies offer 3D printing services in a wide variety of materials and at various print qualities. As *in vivo* imaging modalities become more widespread in ecological research, researchers will have to solve the basic problem of how to hold their particular study species safely and securely for the duration of a PET, CT or MRI scan. Rather than "reinventing the wheel," for each new species, we hope researchers can learn from the design of the AID and use our CAD models as a starting point for fabricating devices for their particular imaging needs.

Acknowledgements

Thanks to the Yale Center for Engineering Innovation and Design for providing access to the 3D printers used in this study. Thanks to D. Keniston, R. Ma and K. Fontaine for helping with the design of the AID, and with issues related to the Inveon scanner. CRL was funded through a Howard Hughes Medical Institute Fellowship of the Life Sciences Research Foundation and a Graduate Women In Science Fellowship.

Appendix A. Supplementary data

Supplementary data associated with this article can be found, in the online version, at https://doi.org/10.1016/j.jneumeth.2017.10.005.

References

Boas, F.E., Fleischmann, D., 2012. CT artifacts: causes and reduction techniques. Imaging Med. 4, 229–240.

Brainard, M.S., Doupe, A.J., 2013. Translating birdsong: songbirds as a model for basic and applied medical research. Annu. Rev. Neurosci. 36, 489–517.

Cheng, T.E., Yoder, K.K., Normandin, M.D., Risacher, S.L., Converse, A.K., Hampel, J.A., Miller, M.A., Morris, E.D., 2009. A rat head holder for simultaneous scanning of two rats in small animal PET scanners: design, construction, feasibility testing and kinetic validation. J. Neurosci. Methods 176, 24–33.

Cross, D.J., Marzluff, J.M., Palmquist, I., Minoshima, S., Shimizu, T., Miyaoka, R., 2013. Distinct neural circuits underlie assessment of a diversity of natural dangers by American crows. Proc. R. Soc. B 280, 20131046.

Doty, F.D., Entzminger, G., Kulkarni, J., Pamarthy, K., Staab, J.P., 2007. Radio frequency coil technology for small-animal MRI. NMR Biomed. 20, 304–325.

Friedman, T., Michalski, M., Goodman, T.R., Brown, J.E., 2016. 3D printing from diagnostic images: a radiologist's primer with an emphasis on musculoskeletal imaging-putting the 3D printing of pathology into the hands of every physician. Skelet. Radiol. 45, 307–321.

Gold, M.E.L., Schulz, D., Budassi, M., Gignac, P.M., Vaska, P., Norell, M.A., 2016. Flying starlings, PET and the evolution of volant dinosaurs. Curr. Biol. 26, R265–267.

Heiss, E., Natchev, N., Salaberger, D., Gumpenberger, M., Rabanser, A., Weisgram, J., 2010. Hurt yourself to hurt your enemy: new insights on the function of the bizarre antipredator mechanism in the salamandrid Pleurodeles waltl. J. Zool. 280, 156–162.

Herrmann, K.H., Gartner, C., Gullmar, D., Kramer, M., Reichenbach, J.R., 2014. 3D printing of MRI compatible components: why every MRI research group should have a low-budget 3D printer. Med. Eng. Phys. 36, 1373–1380.

Kessler, R.M., Ellis Jr., J.R., Eden, M., 1984. Analysis of emission tomographic scan data: limitations imposed by resolution and background. J. Comput. Assist. Tomogr. 8, 514–522.

Lammertsma, A.A., Hume, S.P., 1996. Simplified reference tissue model for PET receptor studies. Neuroimage 4, 153–158.

Lattin, C.R., Pechenenko, A.V., Carson, R.E., 2017a. Experimentally reducing corticosterone mitigates rapid captivity effects on behavior, but not body composition, in a wild bird. Horm. Behav. 89, 121–129.

Lattin, C.R., Stabile, F.A., Carson, R.E., 2017b. Estradiol modulates neural response to conspecific and heterospecific song in female house sparrows: an in vivo positron emission tomography study. PLoS One 12, e0182875.

Levene, H., 1960. Robust tests for equality of variances. In: Olkin, I. (Ed.), Contributions to Probability and Statistics. Stanford University Press, Palo Alto, CA, pp. 278.

Louder, M.I., Voss, H.U., Manna, T.J., Carryl, S.S., London, S.E., Balakrishnan, C.N., Hauber, M.E., 2016. Shared neural substrates for song discrimination in parental and parasitic songbirds. Neurosci. Lett. 622, 49–54.

Marzluff, J.M., Miyaoka, R., Minoshima, S., Cross, D.J., 2012. Brain imaging reveals neuronal circuitry underlying the crow's perception of human faces. Proc. Natl. Acad. Sci. 109, 15912–15917.

Novakova-Marcincinova, L., Novak-Marcincin, J., 2013. Experimental testing of materials used in fused deposition modeling rapid prototyping technology. Adv. Mater. Res. 740, 597–602.

Rich, E.L., Romero, L.M., 2005. Exposure to chronic stress downregulates corticosterone responses to acute stressors. Am. J. Physiol. Regul. Integr. Comp. Physiol. 288, R1628–1636.

Riemann, B., Schäfers, K.P., Schober, O., Schäfers, M., 2008. Small animal PET in preclinical studies: opportunities and challenges. Q. J. Nucl. Med. Mol. Imaging 52, 215–221.

Rogers, L., 1996. Behavioral, structural and neurochemical asymmetries in the avian brain: a model system for studying visual development and processing. Neurosci. Biobehav. Rev. 20, 487–503.

Schambach, S.J., Bag, S., Schilling, L., Groden, C., Brockmann, M.A., 2010. Application of micro-CT in small animal imaging. Methods 50, 2–13.

Souza, M.J., Wall, J.S., Stuckey, A., Daniel, G.B., 2011. Static and dynamic (18)FDG-PET in normal hispaniolan Amazon parrots (*Amazona ventralis*). Vet. Radiol. Ultrasound 52, 340–344.

Van Meir, V., Verhoye, M., Absil, P., Eens, M., Balthazart, J., Van der Linden, A., 2004. Differential effects of testosterone on neuronal populations and their connections in a sensorimotor brain nucleus controlling song production in songbirds: a manganese enhanced-magnetic resonance imaging study. Neuroimage 21, 914–923.

Van Meir, V., Boumans, T., De Groof, G., Van Audekerke, J., Smolders, A., Scheunders, P., Sijbers, J., Verhoye, M., Balthazart, J., Van der Linden, A., 2005. Spatiotemporal properties of the BOLD response in the songbirds' auditory circuit during a variety of listening tasks. Neuroimage 25, 1242–1255.

Van der Linden, A., Van Meir, V., Boumans, T., Poirier, C., Balthazart, J., 2009. MRI in small brains displaying extensive plasticity. Trends Neurosci. 32, 257–266.

Visser, E.P., Disselhorst, J.A., Brom, M., Laverman, P., Gotthardt, M., Oyen, W.J., Boerman, O.C., 2009. Spatial resolution and sensitivity of the Inveon small-animal PET scanner. J. Nucl. Med. 50, 139–147.

Williams, T.D., 2008. Individual variation in endocrine systems: moving beyond the 'tyranny of the Golden Mean'. Phil. Trans. R. Soc. B: Biol. Sci. 363, 1687–1698.

Yagi, M., Arentsen, L., Shanley, R.M., Hui, S.K., 2014. High-throughput multiple-mouse imaging with micro-PET/CT for whole-skeleton assessment. Phys. Med. 30, 849–853.